Neoplasia • Vol. 6, No. 6, November/December 2004, pp. 697–704 697

www.neoplasia.com

A Mathematical Investigation of the Multiple Pathways to Recurrent Prostate Cancer: Comparison with Experimental Data

Trachette L. Jackson

Department of Mathematics, 525 E. University, University of Michigan, Ann Arbor, MI 48109-1109

Abstract

Considerable research is aimed at determining the mechanisms by which hormone-refractory prostate cancer develops. In an effort to assist in the understanding of recurrent prostate cancer and the cellular processes that mediate this disease, a mathematical model is presented that describes both the pretreatment growth and the posttherapy relapse of human prostate cancer xenografts. Our goal is to evaluate the interplay between the multiple mechanisms that have been postulated as causes of androgen-independent relapse. Simulations of the model show that molecular events that render the androgen receptor irrelevant to disease progression, such as upregulation of BCL2, can result in relapse after androgen deprivation therapy. However, decreased apoptosis of androgen-independent cells alone overestimates the effects of hormone therapy when compared to experimental data. When decreased apoptosis is combined with continual androgen receptor activation, the posttherapy growth dynamics are in excellent correlation with experimental observations of the growth of LuCaP xenografts. Furthermore, the mathematical model predicts that upregulation of the androgen receptor, together with its increased activation, is alone sufficient to result in the androgen-independent growth of LNCaP xenografts. Recent experimental studies that suggest that the posttherapy increase in and continual activation of the androgen receptor are common and crucial features of recurrent prostate cancer provide validation of the model predictions. This approach provides a framework for using mathematical techniques to study novel therapeutic strategies aimed at controlling this disease.

Neoplasia (2004) **6,** 697–704

Keywords: Mathematical model, prostate cancer, androgen-independent relapse, LuCap, LNCaP.

Introduction

For American men over the age of 40, prostate cancer is now the most commonly diagnosed cancer and the second leading cause of cancer-related deaths [1]. Prognosis is generally favorable for most early-detected cases of localized prostate cancer. However, in some patients, the disease is very aggressive and even the initial diagnosis shows signs of invasion and metastasis [2]. For this advanced stage of disease, the cornerstone of treatment is androgen deprivation therapy (ADT), a type of hormone therapy in which the body is deprived of androgens through surgical or chemical castration [3–6]. ADT ceases androgen production from its primary source, the testes; however, this does not ensure its elimination from the plasma and body tissues. A small amount is produced by a secondary source, the adrenal glands, and this fount may not be affected by surgical or chemical castration [4]. Although most patients have a positive initial response to ADT, this is usually temporary. Unfortunately, the prognosis is still unfavorable due to the acquisition of an androgen-independent (AI) phenotype that is resistant to secondary endocrine therapy and to chemotherapy [6,7]. At the present time, there is no effective therapeutic option for or clear understanding of the causes of hormone-refractory prostate cancer.

The postulated mechanisms to explain AI relapse include amplification or mutation of the androgen receptor gene (AR), ligand-independent activation of the androgen receptor and alternate signaling pathways, which bypass the growth-promoting functions of the androgen receptor [4,8,9]. Many alterations in the AR have been detected in prostate cancers and a subset of these effect the ligand specificity of the receptor, permitting its activation by nonandrogens or even antiandrogens [10]. This gain of function of the androgen receptor can result in hormone-resistant prostate cancer through the acquisition of AI mechanisms for activation of the androgen receptor [11]. Most patients do not have AR mutations or amplifications, yet they retain active androgen receptor signaling after therapy. Ligand-independent routes to receptor activation could potentially result from increased protein kinase signaling, mediated by oncogenes [12]. Another possible cause of hormone resistance is that the growth-regulatory effects of the androgen receptor can be overridden by alternative, androgen

Abbreviations: AD, androgen-dependent; ADT, androgen deprivation therapy; AI, androgen-independent; AR, androgen receptor; NSE, neuron-specific enolase

Address all correspondence to: Trachette L. Jackson, Department of Mathematics, 525 E. University, University of Michigan, Ann Arbor, MI 48109-1109. E-mail: tjacks@umich.edu

Received 30 March 2004; Revised 15 June 2004.

DOI 10.1593/neo.04259

receptor–independent signaling pathways such as the overexpression of the antiapoptotic protein BCL2 [12,13].

In an effort to understand the biologic characteristics of hormone-refractory prostate cancer, several experimental model systems have been derived. Currently, however, only a few models exist that exhibit the features of human prostate cancer growth [6]. In 1996, Ellis et al. [14] characterized a novel, androgen-sensitive, human prostate cancer xenograft, LuCaP 23. The LuCaP 23 xenografts were developed from human prostatic cancer metastases harvested at autopsy and propagated in athymic mice. These cells secrete large amounts of prostate-specific antigen (PSA) and exhibit many of the characteristics of clinical prostatic carcinoma, including the resumption of growth after ADT. Subsequent studies found that LuCaP 23.1 is composed of at least two tumor cell populations representing two different phenotypes: one is neuron-specific enolase (NSE) positive and the other is NSE negative [13]. Furthermore, the NSE-positive tumors, which were recovered after AI relapse in castrated hosts, also expressed BCL2, a gene product known to inhibit apoptosis. More recently, Chen et al. [12] found that hormone-refractory LuCaP tumors had more androgen receptor protein than their parental hormone-sensitive counterparts. This suggests that multiple mechanism for the acquisition of AI prostate cancer may be at work.

In this paper we present the first experimentally driven mathematical model designed to investigate interplay between the possible mechanisms of AI relapse. Comparing the model to the experimental data of LuCaP 23 xenografts shows that increased BCL2 expression, which inhibits apoptosis in AI cells, can result in AI relapse but in a way that is incompatible with the experimental data. However, combining decreased apoptosis with continued proliferation of a subset of androgen-dependent (AD) cells results in tumor relapse, which is consistent with experimental observations. These results suggest that the continual posttherapy activation of the androgen receptor is a crucial component of recurrent prostate cancer associated with the LuCaP xenografts. Furthermore, blocking the upregulation of the androgen receptor and thereby reducing the proliferation of AD cells could lead to significantly longer remissions.

We also compare the mathematical model to experimental data presented in Ref. [12] for the growth of LNCaP tumors in castrated mice. In this case, the model agrees with the experimental evidence that increased androgen receptor activation alone is sufficient to result in hormone-refractory tumor growth.

Methods

The goal of this study is to test the leading hypotheses for AI relapse through the development and simulation of a mathematical model that describes prostate tumor growth before and after hormone therapy. The tumor is viewed as a densely packed, radially symmetric sphere of radius $R(t)$. Cell movement is produced by the local volume changes that accompany cell proliferation and death. The spheroid expands or shrinks at a rate that depends on the balance between cell growth and division and cell death within the tumor volume, the former and latter being meditated by the presence of androgen, $a(r, t)$.

Tumor Growth Model

Prostatic cancer cells, like the normal prostatic cells from which they arise, are sensitive to androgen stimulation of their growth. The presence of androgen stimulates the daily proliferation of these AD cells while inhibiting their daily percentage of apoptotic death [7,15]. Therefore, before treatment continuous net growth occurs. In contrast, after ADT, the proliferation rate of AD cells is significantly reduced and the rate of cellular suicide is increased [7,15,16]. This results in a decline in the number of AD cells within the tumor and an initial positive response. However, in many prostate micrometastases there is also a heterogeneous presence of AI cancer cells whose proliferation rate exceeds their apoptotic death rate even after total androgen blockage is performed [7]. In the LuCaP 23 experiments, AI cells were undetectable before therapy [14]. After ADT, AI cells, which are characterized as being NSE-positive and containing large quantities of BCL2, were harvested [13].

Based on these findings, we first consider a polyclonal tumor consisting of a heterogeneous mix of two cells types (AD and AI, with AI cells being below detectable levels initially) as the mechanism by which AI relapse can occur. The governing equations for the tumor cell populations are derived by applying the principle of conservation of mass to each phenotype. For solid tumor growth, it is widely assumed that cell movement has two components: 1) net collective motion due to the velocity generated by cell growth and death [17–20] and 2) random motility [18–22]. Based on these assumptions, statements of balance may be written as follows for AD cells, p, and AI cells, q.

$$\frac{\partial p}{\partial t} + \nabla \cdot (\mathrm{u}p) = D_p \Delta p + \alpha_p(\mathrm{a})p - \delta_\mathrm{p}(\mathrm{a})p, \quad (1)$$

Time rate of change of AD cells	+	Collective cellular motion	=	Random cellular motion	+	Androgen-mediated proliferation	−	Androgen-mediated apoptosis

$$\frac{\partial q}{\partial t} + \nabla \cdot (\mathrm{u}q) = D_q \Delta q + \alpha_q(\mathrm{a})q - \delta_\mathrm{q}(\mathrm{a})q, \quad (2)$$

Time rate of change of AI cells	+	Collective cellular motion	=	Random cellular motion	+	Androgen-mediated proliferation	−	Androgen-mediated apoptosis

In Equations (1) and (2) D_p and D_q are the assumed constant random motility coefficients of the two types of tumor cells and $\alpha_p(a)$, $\alpha_q(a)$, $\delta_p(a)$, and $\delta_q(a)$ are their respective proliferation and programmed death rates. These cell proliferation and apoptotic rates are crucially dependent on

the local androgen concentration, $a(r, t)$, and their specific characteristics will be discussed in detail in the hormonal effects subsection to follow.

To assess the tumor's response to ADT it will be important to follow the evolution of the tumor volume (= $4/3\pi R^3$, for radial symmetry) or, equivalently, the tumor radius $R(t)$. We do this by noting that under radial symmetry, the tumor radius expands at a rate that is equal to the radial component of the velocity there, i.e.,

$$\frac{dR}{dt} = u(R(t), t), \quad (3)$$

Time rate of change of the tumor radius = Tumor velocity at the tumor boundary

An equation for the tumor velocity is obtained by adding Equations (1) and (2) with the additional constraint that there are no voids within the tumor so that $p + q = 1$. Implied by this model formulation is that we begin with a tumor of given initial cell density, p_0, q_0; radius, R_0; and androgen concentration, a_0. By symmetry, at the center of the tumor ($r = 0$) there is no flux of androgen and the local velocity is zero. Finally, for the tumor cell populations, we impose no flux of p and q at the tumor center and on its outer boundary.

Androgen Levels

The androgen levels within the tumor are assumed constant until the time of treatment. ADT results in the partial blockage of androgen production and the tumor levels will rapidly decrease to a new, significantly lower, steady state.

Hormonal Effects

The exponential decline of androgen after ADT causes an increase in the apoptotic death rate of AD cells and a decrease in their proliferation [7,16]. A further consequence of therapy is a decrease in the apoptotic rate of AI cells with no significant difference in their proliferation rate when compared to untreated tumor cells [7]. The effect of androgen on proliferative and apoptotic activity is thus modeled by giving the growth and death rates $\alpha_p(a)$, $\alpha_q(a)$, $\delta_p(a)$, and $\delta_q(a)$ these experimentally determined characteristics. Figure 1 illustrates how cell kinetics varies with androgen availability.

The function $\alpha_p(a)$ is chosen so that when androgen is in excess, AD cells proliferate at constant rate, α_1. After ADT, the androgen levels drop quickly and cells proliferate at a fraction of their pretreatment value, $\alpha_1\theta_1$, where θ_1 represents the growth rate in the absence of androgen relative to its value when androgen is abundant. In keeping with experimental observations [7], the function $\alpha_q(a)$ is chosen so that androgen concentration has no effect on the proliferation rate of the AI cells; in other words $\alpha_q(a) = \alpha_2 \equiv$ constant.

The functions $\delta_q(a)$ and $\delta_q(a)$ also suggest that when the androgen supply is plentiful, the cells die at rates δ_1 and δ_2, respectively. When androgen levels fall, the death rate of the AD cells increases to the higher rate $\delta_1\omega_1$. However, in low-androgen environments, increased BCL2 renders the AI cells less susceptible to apoptosis and their death rate decreases to $\delta_2\omega_2$. The parameters ω_1 and ω_2 represent the respective death rates in the absence of androgen relative to their values when androgen is abundant. Based on experimental evidence [7,13], we assume that $\omega_q < 1$ and $\omega_p > 1$. Because AD cells are dominant when androgen is

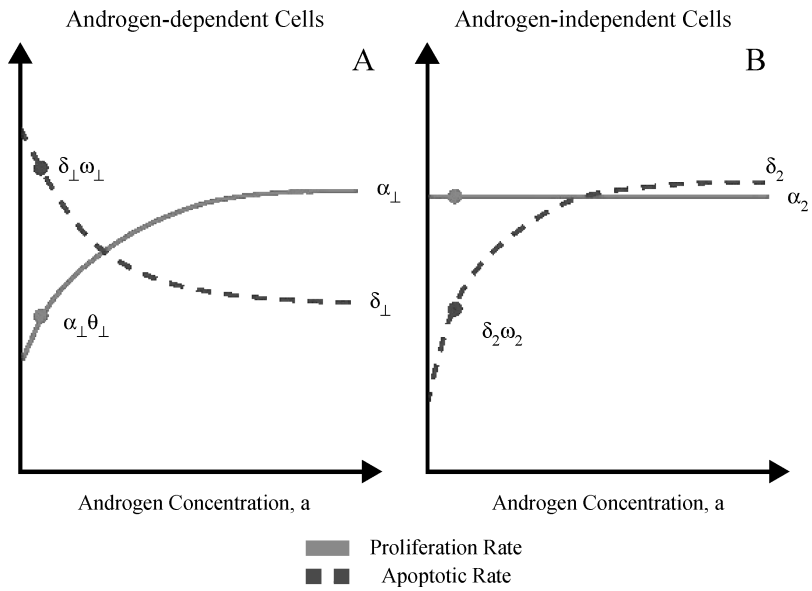

Figure 1. *The effect of androgen concentration on the proliferation and apoptotic rates of AD cells (A) and AI cells (B). The circles indicate posttherapy androgen concentrations and the respective proliferation and death rates.*

abundant [7,14], we will assume $\alpha_1 \approx \alpha_2$, $\delta_1 < \delta_2$, and $\alpha_2 < \delta_2$. This last inequality assures that AI cells are below detectable levels before therapy is initiated (see Figure 1).

Where possible, we make use of published data for the treatment of athymic mice that have been implanted with human prostate cancer xenograft LuCaP 23.1. For those parameters for which no experimental data are available, the goal is to quantify their influence on the model behavior. Table 1 lists each parameter, its baseline value, and source.

Results

Numerical Simulations

Numerical simulations of Equations (1)–(3) are performed to investigate the tumor's response to ADT for various parameter values. The fit of the mathematical model to the experimental data [14] for intact male mice bearing LuCaP 23.1 xenografts is shown in Figure 2. The proliferation rate, $\alpha_1 = 0.4621$ per day, is based on the cells dividing once every 36 hours; therefore, the best fit of the model to this data allows for the estimation of the apoptotic rate, $\delta_1 = 0.3812$ per day. Together, these parameters result in a tumor-doubling time of 8.6 days.

The range of behaviors the model can exhibit once ADT has been initiated is depicted in Figure 3*A*. All parameters are taken from Table 1 with $\omega_1 = 1.35$ and ω_2 varying between 0.25 and 1.0. In these simulations, polyclonality and decreased apoptosis of AI cells are the only operative mechanisms for tumor relapse. In other words, the increased activation of the androgen receptor (through amplification other pathways) is not considered here as evidenced by the negative net growth rate of the AD cells. The model predicts that for certain parameter values, ADT can result in control

Table 1. List of Baseline Parameter Values Used in Simulations and Their Sources.

Parameter	Value	Reference
α_1	0.4621 d^{-1}	[7]*
α_2	0.4621 d^{-1}	[7]†
δ_1	0.3812 d^{-1}	Best fit to data of Ellis et al. [14]
δ_2	0.4765 d^{-1}	[7]‡
θ_1	0.8	
ω_1	1.18–1.35	Best fit
ω_2	0.25–1.0	Best fit
P_0	0.995	[8]§
D_p	10^{-10} cm^2 s^{-1}	[24]
D_q	10^{-10} cm^2 s^{-1}	[24]

*Berges et al. [7] report that malignant prostatic cells from five different patients had an average cell cycle time of 48 ± 5 hours. Proliferation rate varies with cell line; we therefore base this parameter on cells dividing once every 36 hours.

† Berges et al. [7] noted no significant change in the proliferation rate of AI cells when compared with metastatic cancer cells in untreated hosts.

‡ Berges et al. [7] noted a two-fold increase in the percentage of AI cells dying per day when compared to metastatic cancer cells in untreated hosts. We modified this to a 25% increase in the apoptotic rate, which is sufficient result in the exponential decline of any initial population of AI cells.

§ Based on the observation that AI cells were not detectable before ADT [14].

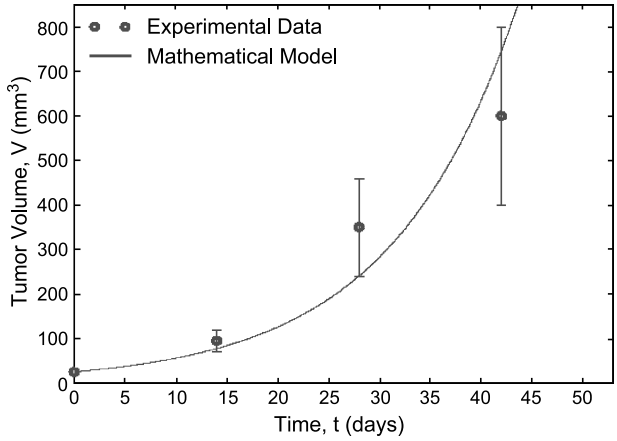

Figure 2. *Best fit of mathematical model of tumor volume versus time to the experimental data of [14]. Given the proliferation rate listed in Table 1, this simulation was used to estimate the apoptotic rate of the AD cells, δ_p.*

of the tumor or in AI relapse. Notice that when ω_2, which represents the amount by which the apoptotic rate is reduced in the absence of androgen, is equal to unity (corresponding to no decreased apoptosis of AI cells) the tumor regresses. As ω_2 increases, corresponding to an increase in BCL2 expression and decreased apoptosis, the model predicts that the tumor response to therapy ranges from prolonged remission ($\omega_2 = 0.75$) to rapid relapse ($\omega_2 = 0.25$). Furthermore, the androgen-sensitive period is always characterized by a marked decrease in tumor volume and both the rate of posttherapy tumor growth and the time of relapse increase and ω_2 decreases.

Figure 3*B* highlights the phases of tumor growth before and after ADT with $\omega_2 = 0.5$. From this simulation, it is evident that the model captures the exponential pretreatment tumor growth, the transient androgen-sensitive period immediately after treatment, and the return to exponential growth in the absence of androgen.

Further information regarding tumor growth and the mechanism for relapse can be gleaned from Figure 4 where the temporal variations in the proliferative activity and apoptotic activity are plotted. These quantities are defined as the total cellular proliferation (or death) within the tumor:

$$\text{Proliferative activity} = \alpha_p(a)p + \alpha_q(a)q \tag{4}$$

$$\text{Apoptotic activity} = \delta_p(a)p + \delta_q(a)q$$

From Figure 4, it is clear that there are specific times for which proliferative activity exceeds apoptotic activity, resulting in net growth. During the androgen-sensitive period, the apoptotic activity surpasses the proliferative activity resulting in tumor regression. The model also predicts that AI relapse is associated with a decrease in apoptotic activity without an increase in proliferation. This result is in agreement with experimental observations, which found that whereas the BUdR index remained at 50% of the pretherapy value for

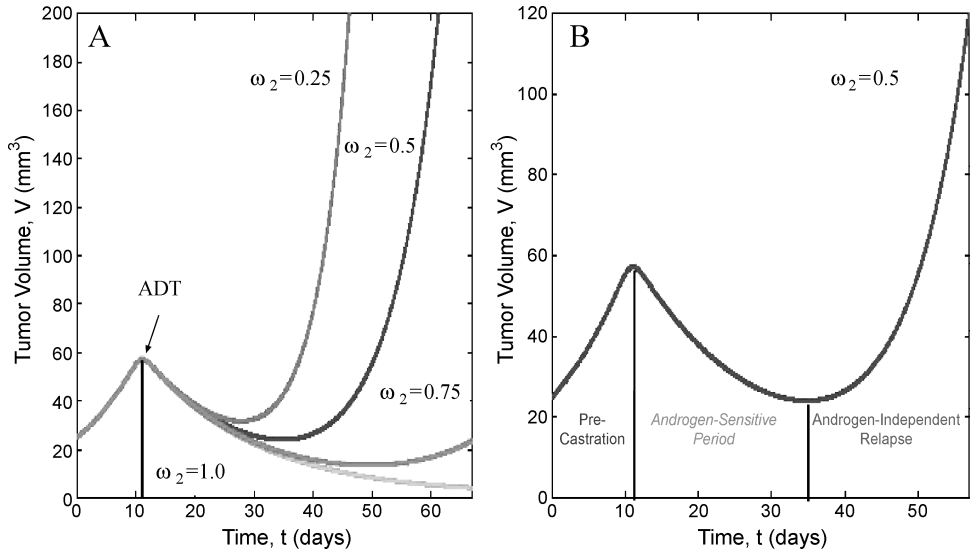

Figure 3. *Plot of tumor volume versus time before and after ADT as predicted by the mathematical model. In (A), the relative death rate of AI cells in the absence of androgen (ω_2) is varied from 0.25 to 1.0. Tumor growth dynamics range from rapid relapse to prolonged remission or complete regression. (B) Highlights the case when ω_2 = 0.5 and illustrates the exponential tumor growth before treatment, the transient androgen-sensitive period immediately after ADT, and the eventual AI relapse.*

days 28 to 112, there was a progressive decrease in the apoptotic index [16].

Comparison with Experimental Data

LuCaP Xenografts Figure 5 compares the mathematical model to experimental data [10] that exhibits three types of responses to therapy. For the minimal and intermediate responses, the best fit parameters are associated with a 15% decrease net proliferation of AD cells (or equivalently, an 18% increase in the apoptotic rate) and a 40% and 60% decrease in the apoptotic rate of the AI cells (ω_2 = 0.6, 0.4, respectively). The best fit for the prolonged response corresponds to a 20% increase apoptotic rate of the AD cells with no decrease in the apoptotic rate of the AI cells.

There is an interesting conclusion that can be drawn based on the parameters used in Figure 5 to fit the experimental data. First, note that in all cases the net growth rate of the AD cells is substantially lower than the precastration value; however, it is still positive. In fact, it is impossible to fit the data when ADT results in complete clearance of the AD cells. The implication of this result is that some amount of continual proliferation of the AD cells, even in the absence androgen, occurs. This is consistent with some mechanism of continual AR activation (whether by AR amplification or by other pathways), and is required to match the experimental data of Ellis et al. [14].

A comparison of the mathematical model and the experimental data of Bladou et al. [16] is given in Figure 6. These data show that ADT induced a significant decrease in the

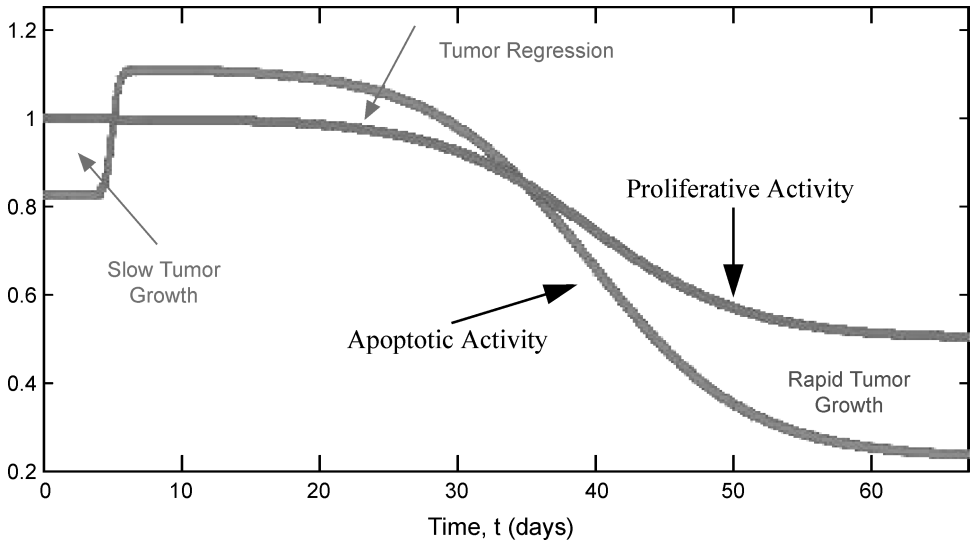

Figure 4. *Plot of the tumor's proliferative and apoptotic activity versus time.*

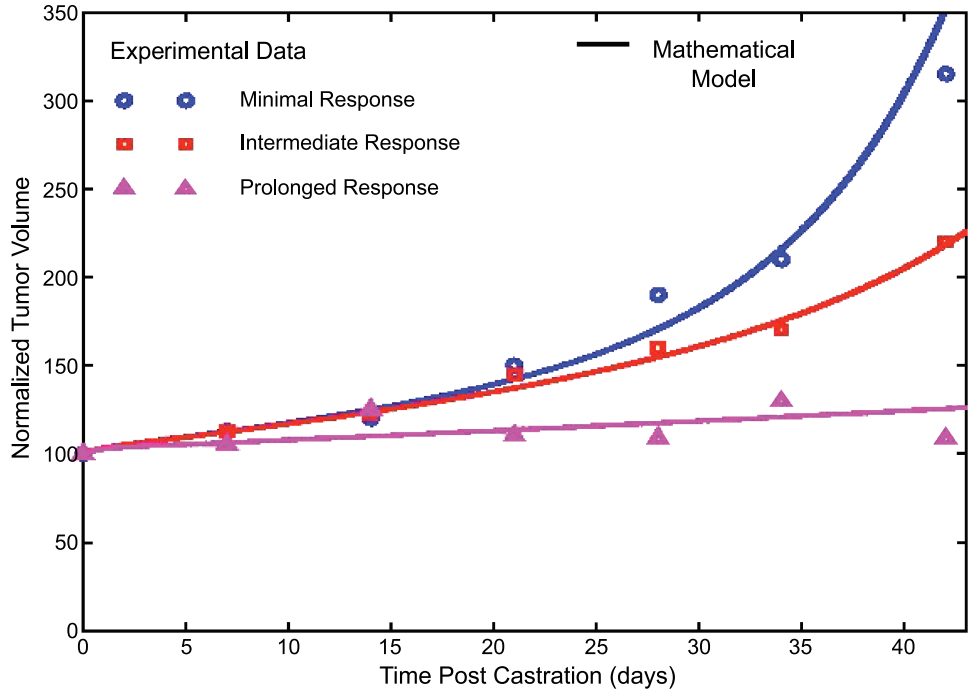

Figure 5. *Best fit of the mathematical model to the experimental data of Ellis et al. [14] for normalized tumor volume versus time post-ADT.*

tumor growth rate for the first 7 days postcastration and a progressive increase thereafter. In Figure 5, $\omega_2 = 1.19$ and $\omega_2 = 0.6$, which again suggests the continual proliferation of AD cells even when androgen levels are low.

LNCaP Xenografts Figure 6 compares the mathematical model to experimental data of Chen et al. [12] for the growth of LNCaP cells in castrated mice. For these simulations, we have removed the assumption that the tumor is comprised of cells that are BCL2-positive. Therefore, the only mechanism for hormone-refractory tumor growth is upregulation and increased activation of the androgen receptor. The mathematical model predictions are very close to the experimental data and highlight the fact that upregulation

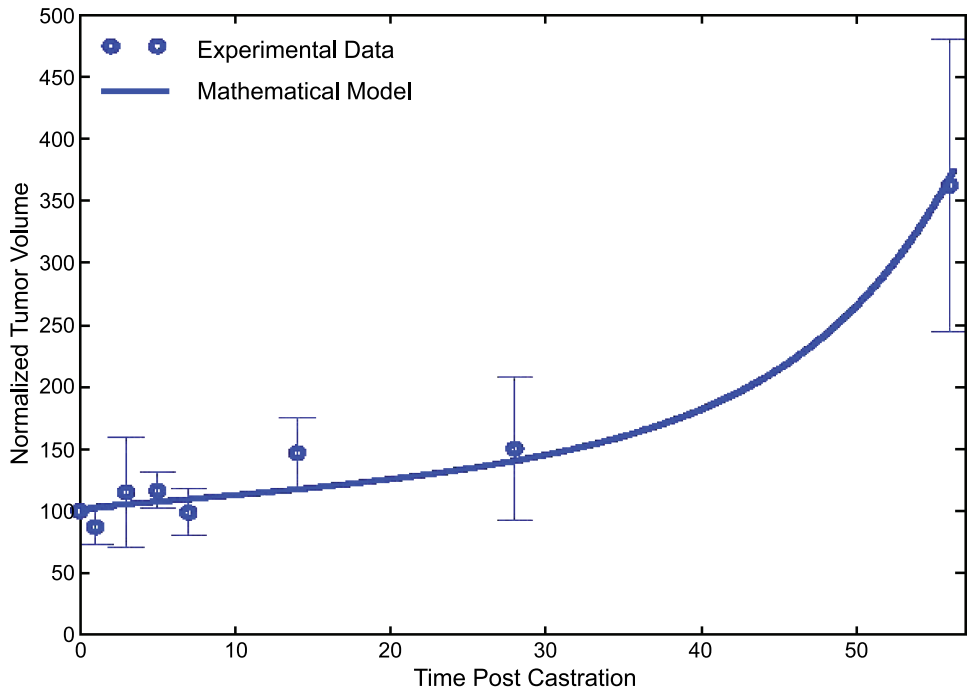

Figure 6. *Best fit of the mathematical model to the experimental data of Bladou et al. [16] for normalized tumor volume versus time post-ADT.*

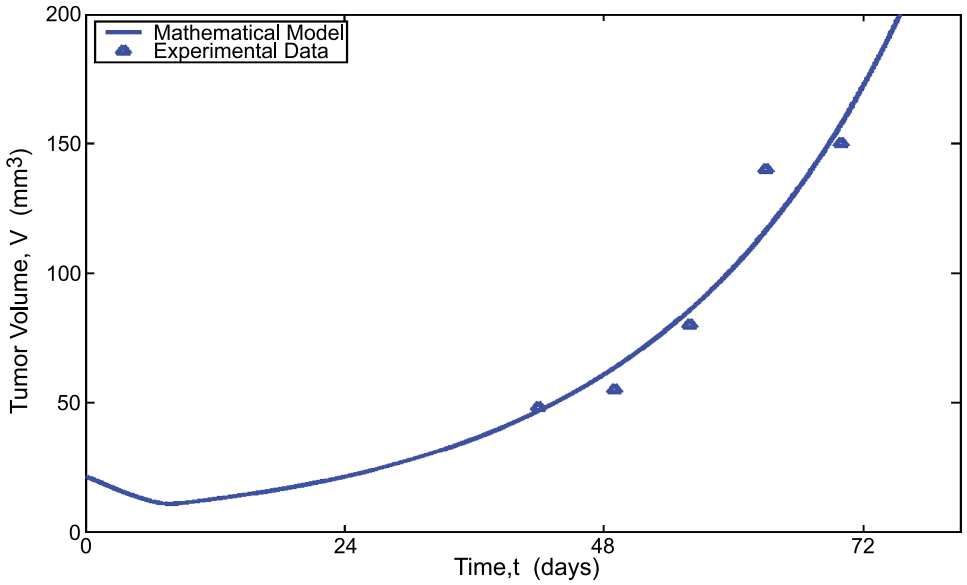

Figure 7. *Comparison of the mathematical model to the experimental data of Chen et al. [12] for tumor volume versus time in castrasted mice implanted with LNCaP tumor xenogarfts. In thse experiments tumor size was measured weakly and scored positive when size reached 40mm^3.*

of the androgen receptor is sufficient to cause AI tumor growth.

Discussion

The question of whether AI growth of prostate cancer is due to adaptation of AD cells (by amplification of the androgen receptor or some other mechanism) or to clonal selection of AI cells is yet unanswered. In an effort to assist in the understanding of hormone-refractory prostate cancer and mechanisms that possibly mediate this disease, we propose a mathematical model that describes both the pretreatment growth and the eventual post-ADT relapse of human prostate cancer xenografts (LuCaP 23 and LNCaP). Simulations of the model with polyclonality and decreased apoptosis of the AI cells predict that for certain parameter values, ADT can result in prolonged remission of the tumor or in AI relapse. In agreement with experimental observations, the relapse is associated with decrease in apoptotic activity without an increase in proliferation. The mathematical model predicts that this mechanism alone overestimates the tumor reduction during the androgen-sensitive period and is incapable of matching the experimental data for tumor volume as a function of time post-ADT. This overestimation suggests that factors that allow for the survival of some fraction of AD cells may also be operative and highlights the importance of eliminating the continual proliferation of AD cells after therapy.

Another potentially crucial factor associated with hormone-refractory cancer is increased androgen-receptor activation [4,9,12–15,23], which could allow for the reduced but continual proliferation of AD cells even when androgen levels are suboptimal. In fact, Chen et al. [12] recently found that an increase in androgen receptor mRNA was the only change that could be consistently associated with the development of hormone resistance across seven human prostate cancer xenografts (LuCaP and LNCap included). When parameters of the model are changed to allow for effects of upregulation and increased receptor activation in combination with decreased apoptosis, simulations show that the two mechanisms together agree with the LuCaP experimental data. These results imply that both increased BCL2 expression in AI cells and increased androgen receptor activation in AD cells may contribute to the recurrent growth of LuCaP 23 xenografts.

When the mathematical model is compared with the experimental data for hormone-insensitive LuCaP xenografts, there is no need to include mechanisms that bypass the functional importance of the androgen receptor. The model prediction agrees with experimental observations that upregulation and increased receptor activation is sufficient to result in AI tumor growth.

The model presented here is a preliminary study of possible causes of the continued growth of prostate cancer after ADT. The possibility of adaptation of AD cells is considered by changing the parameters of this model to describe the continual proliferation of AD cells in the androgen-depleted conditions occur posttherapy. A future investigation will modify and extend this model to describe the specific adaptation of AD cells by particular pathways, including gain of function of the androgen receptor [10], which result in increased receptor activation in response to low androgen levels. Such an investigation will assist in determining which mechanisms of receptor activation, alone and in combination, lead to relapse that is consistent with experimental data. The mathematical model described in this paper and the extensions alluded to above provide a quantitative method for studying the possible causes of AI prostate cancer growth and can be used to test novel therapeutic strategies targeted at hormone-refractory prostate cancer.

Acknowledgements

The author thanks James D. Murray, FRS, and Lawrence D. True, MD, for bringing forth this idea for interdisciplinary modeling. Additional thanks to Nicholas Britten, PhD, Patrick Nelson, PhD, Paul Kulesa, PhD, and Patricia Burgess, MSc, for their helpful discussions and preliminary modeling ideas.

References

[1] Greenlee RT, Murray T, Bolden S, and Wingo PA (2000). Cancer statistics 2000. *CA Cancer J Clin* **50,** 7–33.

[2] Crawford ED, Rosenblum M, Ziada AM, and Lange PH (1999). Hormone refractory prostate cancer. *Urology* **54** (Suppl 6A), 1–7.

[3] Denis LJ and Griffiths K (2000). Endocrine treatment in prostate cancer. *Semin Surg Oncol* **18,** 52–74.

[4] Palmberg C, Koivisto P, Kakkola L, Tammela TLJ, Kallioniemi OP, and Visakorpi T (2000). Androgen receptor gene amplification at primary progression predicts response to combined androgen blockade as second line therapy for advanced prostate. *J Urol* **164** (6), 1992–1995.

[5] Basaria S, Leib J, Tang AM, DeWeese T, Carducci M, Eisenberger M, and Dobs AS (2002). Long-term effects of androgen deprivation therapy in prostate cancer patients. *Clin Endocrinol (Oxf)* **56** (6), 779–786.

[6] Igawa T, Lin FF, Lee MS, Karan D, Batra SK, and Lin MF (2002). Establishment and characterization of androgen-independent human prostate cancer LNCaP cell model. *Prostate* **50** (4), 222–235.

[7] Berges RR, Vukanovic J, Epstein JI, CarMichel M, Cisek L, Johnson DE, Veltri RW, Walsh PC, and Isaacs JT (1995). Implication of cell kinetic changes during the progression of human prostatic cancer. *Clin Cancer Res* **1,** 473–480.

[8] Rini BI and Small EJ (2002). Prostate cancer update. *Curr Opin Oncol* **14** (3), 286–291.

[9] Gregory CW, Johnson RT, Presnell SC, Mohler JL, and French F (2001b). Androgen receptor regulation of G1 cyclin and cyclin-dependent kinase function in the CWR22 human prostate cancer xenograft. *J Androl* **22** (4), 537–548.

[10] Nelson WG, De Marzo AM, and Isaacs WB (2003). Prostate cancer. *N Engl J Med* **349** (4), 366–381.

[11] Litvinov IV, De Marzo AM, and Isaacs JT (2003). Is the Achilles' heel for prostate cancer therapy a gain of function in androgen receptor signaling? *J Clin Endocrinol Metab* **88** (7), 2972–2982.

[12] Chen CD, Welsbie DS, Tran C, Baek SH, Chen R, Vessella R, Rosenfeld MG, and Sawyers CL (2004). Molecular determinants of resistance to antiandrogen therapy. *Nat Med* **10** (1), 33–39.

[13] Liu AY, Corey E, Bladou F, Lange PH, and Vessella RL (1996). Prostatic cell lineage markers: emergence of $BCL2^+$ cells of human prostate cancer xenograft LuCaP 23 following castration. *Int J Cancer* **65,** 85–89.

[14] Ellis WJ, Vessella RL, Buhler KR, Bladou F, True LD, Bigler SA, Curtis D, and Lange PH (1996). Characterization of a novel androgen-sensitive prostate-specific antigen-producing prostatic carcinoma xenograft: LuCaP 23. *Clin Cancer Res* **2,** 1039–1048.

[15] Gregory CW, Fei X, Ponguta LA, He B, Bill HM, French FS, and Wilson EM (2004). Epidermal growth factor increases coactivation of the androgen receptor in recurrent prostate cancer. *J Biol Chem* **279,** 7119–7130.

[16] Bladou F, Vessella RL, Buhler KR, Ellis WJ, True LD, and Lange PH (1996). Cell proliferation and apoptosis during prostatic tumor xenograft involution and regrowth after castration. *Int J Cancer* **67,** 785–790.

[17] Greenspan HP (1976). On the growth and stability of cell cultures and solid tumors. *J Theor Biol* **56,** 229–235.

[18] Byrne HM and Chaplain MAJ (1996). Modelling the role of cell–cell adhesion in the growth and development of carcinoma. *Math Comput Model* **24** (12), 1–17.

[19] Jackson TL and Byrne HM (2000). A mathematical model to study the effects of drug resistance and vasculature on the response of solid tumors to chemotherapy. *Math Biosci* **164** (1), 17–38.

[20] Jackson TL (2002). Vascular tumor growth and treatment: consequences of polyclonality, competition, and dynamic vascular support. *J Math Biol* **44,** 201–226.

[21] Woodward DE, Cook J, Tracqui P, Cruywagen GC, Murray JD, and Alvord EC (1996). A mathematical model of glioma growth: the effect of extent of surgical resection. *Cell Prolif* **29,** 269–288.

[22] Burgess PK, Kulesa PM, Murray JD, and Alvord EC (1997). The interaction of growth rates and diffusion coefficients in a three-dimensional mathematical model of gliomas. *J Neuropathol Exp Neurol* **56,** 704–713.

[23] Gregory CW, He B, Johnson RT, Ford OH, Mohler JL, French FS, and Wilson EM (2001). A mechanism for androgen receptor-mediated prostate cancer recurrence after androgen deprivation therapy. *Cancer Res* **61** (11), 4315–4319.

[24] Bray D (2001). Cell Movements Garland Publishing, New York, NY.